Proc. Natl. Acad. Sci. USA
Vol. 91, pp. 9965–9969, October 1994
Neurobiology

Visual form discrimination from color or motion cues: Functional anatomy by positron emission tomography

(regional cerebral blood flow/human visual cortex/form)

B. GULYÁS*†, C. A. HEYWOOD‡, D. A. POPPLEWELL‡, P. E. ROLAND*, AND A. COWEY‡

*Laboratory for Brain Research and Positron Emission Tomography, Department of Neuroscience, Karolinska Institute, S-171 77 Stockholm, Sweden; and ‡Department of Experimental Psychology, Oxford University, South Parks Road, Oxford, OX1 3UD, United Kingdom

Communicated by James M. Sprague, June 29, 1994 (received for review February 8, 1994)

ABSTRACT **To explore the extent to which various cortical functional pathways are involved in processing and analyzing different types of information that yield the same perceptual entity, we mapped anatomical structures in the human brain participating in the discrimination of visual forms mediated either by motion or color cues. Changes in regional cerebral blood flow were measured in 10 young male volunteers with positron emission tomography and with [^{15}O]butanol. During the measurements, the subjects performed four visual discrimination tasks (form-from-motion, motion alone, form-from-color, and color alone discrimination). The individual regional cerebral blood flow images were standardized in shape and size with the help of a computerized brain atlas. Subtraction images were determined and averaged across data from all subjects. The resulting images were analyzed for statistically significant changes between specific and reference tasks. The discrimination of form by means of motion cues activated functional fields bilaterally in the inferior and lateral occipital gyri, in the lingual, anterior cingulate, middle frontal and orbitofrontal gyri, and in the left fusiform and right inferior temporal gyri. Form discrimination by color cues resulted in activation bilaterally in the inferior temporal, lateral occipital, and orbitofrontal gyri, the left precuneus and intraparietal sulcus, and the right precentral gyrus. The regions engaged in the two kinds of form discrimination did not overlap, demonstrating that differences in visual forms mediated by color or motion cues are processed and analyzed by disparate networks of functional fields in human cerebral cortex.**

Several physiological observations suggest that neuronal signals about color and motion are processed and analyzed by different functional pathways at early levels in the primate visual system (1–7). Although there are interactions between the systems coding color and motion (8–10), they and their underlying pathways are regarded as initially independent (11, 12). Both the color and motion systems provide signals that can elicit the same categories of visual perceptual entity, such as contour or form.

In monkeys, several studies show that cells sensitive to visual form are located in cortical regions along a "ventral" occipitotemporal visual pathway and it has often been claimed that the detailed analysis of visual forms occurs, in great part, in the inferior temporal cortex (13–17). It has also been shown that there are form-selective neurons in the macaque inferior temporal cortex that are equally activated by visual forms formed by luminance, motion, or texture cues (18). However, claims that there is a center or are centers in the brain [the "form area(s)"] exclusively specialized for the perception of complex forms, such as faces, have recently been challenged by lesion studies in monkeys (19). Furthermore, positron emission tomography (PET) studies in humans using various visual form-related psychophysical paradigms have shown a large number of cortical regions to be active during the different form tasks (20–24).

With the intention of exploring in the human visual system (*i*) whether motion and color are analyzed by identical, overlapping, or different cortical substrata and (*ii*) whether discrimination of visual form mediated by motion and color cues engage the same cortical regions, we measured regional cerebral blood flow (rCBF), as an indicator of regional cerebral metabolism, with PET, using [^{15}O]butanol as tracer, in 10 healthy male volunteers while they performed a series of visual discrimination tasks.

METHODS

Subjects. Ten healthy male volunteers (age, 28.2 ± 2.7 years, mean ± SD) participated. They were fully informed about the objectives, details, and risks of the experiment and gave a written consent, in agreement with the Helsinki Declaration and the Code of Federal Regulations: Protection of Human Subjects (25, 26). The study was approved by the Ethical and Radiation Safety Committees of the Karolinska Hospital. Nine subjects were right handed and one subject was left handed, as assessed by the Edinburgh handedness inventory (27). Seven subjects were emmetropes, and three had appropriate spectacle correction. The subjects' color vision was tested before the experiment using a Velhagen chart (28). None of them had any manifest or hidden color vision or visual field deficit.

Four PET measurements were taken on the subjects while they performed visual discrimination tasks. The tasks were interleaved in different orders in different subjects. During the scan, the subjects were comfortably placed in supine position on the camera bed. With the exception of the ambient noise of the scanners, the electroencephalogram (EEG) apparatus, and the arterial pump, there was no noise in the room, which was kept at 23°C. The auditory environment was not disturbed by any movements or speech by the personnel who were in a remote control room. The subjects were required not to move or activate their muscles, to say anything, or to change the respiratory rhythms after the injection, with the exception of pressing a response key to register their responses with their right middle or index fingers. The visual field of the subjects, including the projection screen, was isolated from the rest of the room by black drapes.

Visual Stimulation. The stimulus displays were presented on a 20-inch color monitor [Microvitec 2038 with a screen

Abbreviations: PET, positron emission tomography; rCBF, regional cerebral blood flow; gCBF, global cerebral blood flow; EEG, electroencephalogram; MR, magnetic resonance; $PaCO_2$, arterial partial CO_2 pressure; PaO_2, arterial partial O_2 pressure; CBA, computerized brain atlas.

†To whom reprint requests should be addressed.

The publication costs of this article were defrayed in part by page charge payment. This article must therefore be hereby marked "*advertisement*" in accordance with 18 U.S.C. §1734 solely to indicate this fact.

resolution of 768 × 576 pixels and a viewing distance of 125 cm (1° = 2.2 cm; 1 inch = 2.54 cm)]. The screen subtended 18° × 16°. For each task a horizontal row of three stimuli, separated by 3°, was presented on the screen against a stationary background composed of a yellow [CIE (Commission International d'Éclairage) coordinates: $X = 0.510$; $Y = 0.426$] 10% random pixel pattern. The luminance of the pixels was 10.0 cd/m^2. Form-from-motion and form-from-color discriminations were each paired with their reference tasks, motion discrimination and color discrimination, respectively. For image analysis, the images revealed by the reference task were subtracted from those revealed by the corresponding discrimination task.

The subject had to indicate the odd-one-out, which appeared either to the right or left of the row of stimuli, by pressing one of two buttons. There was no time pressure on the subject and a new trial immediately followed a response. The difficulty of the discrimination was varied from trial to trial. Three consecutive correct responses resulted in a more difficult discrimination. An easier discrimination followed a single error. Predetermined thresholds for each discrimination ensured that the subject's performance during PET measurements tracked his threshold.

In the color discrimination task (Fig. 1), the stimuli were three squares (2.5° × 2.5°) composed of the same random dot pattern as the background. The red and green guns were modulated, while maintaining isoluminance, to define the three squares, two red and one green, or vice versa. The hue difference was titrated by halving or doubling the depth of modulation of the guns, with γ correction, after correct or erroneous responses, respectively. For the form-from-color discrimination, two squares and a rectangle, or vice versa, were presented of identical area. They were either red (CIE coordinates: $X = 0.563$; $Y = 0.390$) or green (CIE coordinates: $X = 0.445$; $Y = 0.484$), at random, and isoluminant with the yellow background that remained constant from trial to trial. The difficulty of the form discrimination was titrated, in the manner described above, by changing the width/height ratio of the rectangle. The relative vertical positions of the three forms were randomly varied from trial to trial to ensure that the odd-one-out was not conspicuous because of the collinearity of the edges of the remaining two.

In the motion-discrimination task, squares were created by random motion of their constituent pixels. From trial to trial, a coherent motion component was added to either one or two of the three squares; i.e., a percentage of the dots all moved to the right or left. The subject was required to indicate the odd-one-out. The percentage of pixels that moved coherently was titrated, as above, and PET measurements were made while subjects tracked threshold. In the form-from-motion task, squares and rectangles were defined by the coherent motion of all their constituent pixels and the form discrimination was identical in other respects to the form-from-color discrimination.

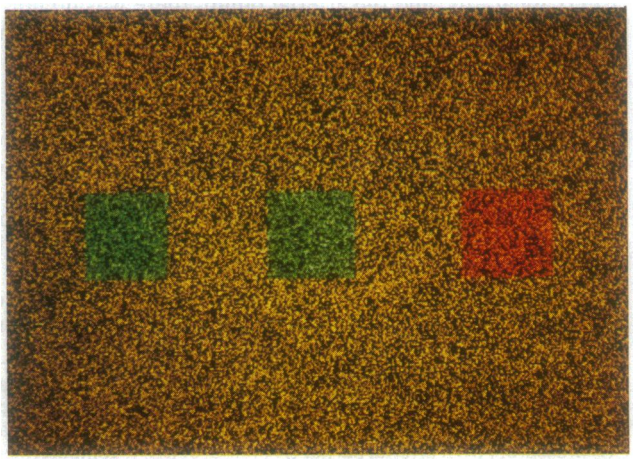

FIG. 1. Stimulus used in the color discrimination task.

Brain Scanning. A high-resolution nuclear magnetic resonance (MR) scan (GE 3514 MR camera, 1.5 Tesla) was made of each brain (both proton-enhanced and T_2-weighted images: spatial resolution, 0.5 mm; slice thickness, 4 mm; interslice distance, 6.5 mm; spin echo, T_R = 2300 msec and T_E = 25 msec and 90 msec). The head fixations in the MR and PET scans were identical (29, 30) so that the corresponding MR and PET images were superimposable. The PET scanning [15 transaxial slices at 6.5 mm (distance)] was made by a Scanditronix PC2048-15B positron emission tomograph, having a 5-mm in-plane spatial resolution (31, 32). [^{15}O]Butanol, a freely diffusible flow tracer, was used to measure rCBF (33). During the experiments EEG, electrooculogram (saccadic eye movements of an amplitude >1 degree), arterial radiotracer concentrations, arterial partial O_2 pressure (PaO_2) and arterial partial CO_2 pressure ($PaCO_2$) levels were continuously monitored. The response latencies and performance levels were calculated on-line. rCBF and global cerebral blood flow (gCBF) measurements were taken during the tasks. Differences in rCBF between the tasks resulting from differences in $PaCO_2$ were corrected (34). Other aspects of the method, including the adequacy of resolution parameters to the present study, were as described (35).

Image Analysis. The MR and PET images were transferred into the computerized brain atlas (CBA) of Bohm and Greitz (36, 37) and transformed into standard size and shape. The contours of the CBA were adjusted to the MR tomograms of the individual brains. Thereafter, the transformation parameters were used to transform the individual PET images into anatomically standardized PET images. Individual difference images ($\Delta rCBF_{\Delta C}$, where ΔC is form-from-color − color discrimination, and $\Delta rCBF_{\Delta M}$, where ΔM is form-from-motion − motion discrimination) were created, which were then averaged across the whole subject population to provide averaged subtraction images ($\Delta rCBF_{ave}$), as well as corresponding descriptive t images ($\Delta rCBF_{ave}/SEM$).

The statistical cluster analysis has recently been described extensively (35); therefore, only a brief description is needed here. From the individual ΔrCBF images, mean ΔrCBF images ($\Delta rCBF_{ave} = \Sigma\, \Delta rCBF/\text{number of subjects}$), variance images, and descriptive Student's t images [$(\Delta rCBF_{ave}/\sqrt{\text{variance}})/\sqrt{\text{number of subjects}}$] were calculated. Voxels in the image (volume, 44 mm^3) having t values ≥ 2.26 were considered to be clustered if they were attached by side, edge, or corner. On the basis of an analysis of false-positive clusters with high t values (35), the hypothesis that all clusters of size 8 and above belong to the distribution of false positives was rejected. The probability of finding one false-positive cluster of size 8 and above in the whole brain was ≤ 0.5, whereas the probability of finding two or three false-positive clusters was ≤ 0.13 or ≤ 0.008, respectively. (Raising the acceptable cluster size to 9 or more to eliminate the false positives could lead to false negatives—i.e., to the omission of positively identified activated fields.) The threshold of the descriptive t image was set to contain only clusters of voxel size 8 or more with voxel values $t \geq 2.26$. The remaining voxel values were set to zero. The resulting image is called a cluster image. In this image all clusters of size 8 and above are shown as regions of significantly changed rCBF. In Table 2 the volumes of regions (together with levels of activation inside the region) are shown.

Localization of Regions. The clusters determined by the statistical procedures were localized in the coordinate system of the CBA and the standardized coordinates of the center of the clusters were also calculated in the Talairach system (38)

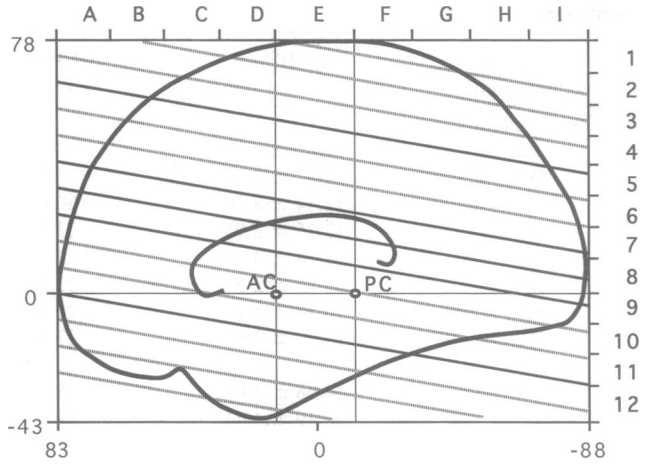

FIG. 2. Talairach proportional stereotactic system and the location of the horizontal MR and PET image slices used in the study. The dashed or solid horizontal lines correspond to the 15-image slices of the MR and PET scans; the button slice is denoted as slice 1, the top one as slice 15. Slices shown in Fig. 3 correspond to the solid oblique lines in the figure. AC, anterior commissure; PC, posterior commissure. Lettering and numbering along the top and right sides represent the original Talairach denotions; figures along the left and bottom sides correspond to millimeter values (38).

(Fig. 2). Regions of activation were outlined on the basis of the cluster image and transferred to the mean ΔrCBF image, where levels of rCBF inside the regions and the center of gravity of the regions were determined. The anatomical names of the regions follow the names of the corresponding region in the CBA as described by Greitz *et al.* (39).

Logic of Paradigm Construction. Out of the four tasks, two tasks were related to form discrimination (form from color and form from motion) and two tasks served as their reference tasks (color discrimination and motion discrimination). Although a form component was present in all tasks, it did not play any role in the reference tasks, as in these tasks the discriminanda were either color or motion within identical forms. On the other hand, the discriminandum in the form discrimination tasks was form created purely by color or motion. By subtracting the corresponding reference tasks from the form tasks, one eliminates components related to the analysis of color or motion, whereas the components related to form discrimination remain in the resulting subtraction images (hereafter called color form or motion form).

RESULTS

Physiological and Response Measurements. There were no significant differences among the tasks with respect to the blood gas levels, α-blockade in the EEG, frequency of saccadic eye movements, and gCBF. Performance levels did not differ significantly between the two motion tasks, though they did between the two color tasks ($P \leq 0.01$) (Table 1).

Activated Regions: Discrimination of Form Mediated by Motion. In the occipital lobe, several disparate fields were bilaterally activated in the lateral and inferior occipital gyri, the lingual gyri, and the left fusiform gyrus. In addition to occipital activations, there were activated fields in the right inferior temporal gyrus, bilaterally in the middle frontal gyri, the anterior cingulate gyri, and the cerebellum (Table 2 and Fig. 3).

Activated Regions: Discrimination of Form Mediated by Color. Activations in this condition were present bilaterally in the fusiform and occipital lateral gyri, the right inferior frontal gyrus, left superior frontal gyrus, the right cingulate and precentral gyri, the left inferior temporal gyrus, cortex lining the left intraparietal sulcus, and left precuneus (Table 2 and Fig. 3).

Overlaps of Activations. Since all cluster images were in the same standard anatomical format, one can by multiplying one image with another image see whether positively identified fields of activation overlap in the brain. By multiplying the color-form cluster image with the motion-form cluster image, we could demonstrate that there were no overlaps of activated fields between the two conditions (Fig. 4).

DISCUSSION

With the aim of mapping those regions of the cerebral cortex participating in the discrimination of visual form based purely upon color or motion cues, we measured rCBF changes with PET. As a result of the subtraction technique, regions involved in both form discrimination tasks and their reference tasks are canceled out. For this reason there is no remaining activation present, for instance, in the primary visual cortex. On the other hand, the subtraction revealed those areas specifically activated when form discrimination was made on the basis of color or motion. There were no overlapping fields present under the two form-discrimination conditions, indicating that the human brain uses different sets of cortical fields during the discrimination of visual forms produced by different visual cues.

The stimulus energies reaching the retina and their spatial distributions were highly similar in all four tasks and there was no significant difference in the tasks with respect to gCBF, $PaCO_2$ and PaO_2 levels, α blockade in the EEG, and eye movement frequencies. These facts indicate that the differences in rCBF between the tasks are related to the specific task components and are not the results of nonspecific components such as differences in eye movement frequency or attentional differences.

The activated regions presumably indicate the distributed cortical networks underlying the percepts of visual forms under different conditions, i.e., the networks involved in submodality-specific form discrimination. The network involved in the discrimination of form based upon color cues involved fewer fields of activation. Compared with our former studies (24), the regions involved in form discrimination on the basis of color cues do not overlap with those involved in color discrimination, indicating that indeed the color component *per se* was eliminated by the subtraction technique. The activated fields are predominantly in the occipital lobe (both fusiform and occipital lateral gyri),

Table 1. Physiological and response measurements during the four tests

	Color discrimination	Shape from color	Motion discrimination	Shape from motion
gCBF, ml per 100 g per min	50.8 ± 14.7	51.9 ± 11.5	48.8 ± 11.6	50.6 ± 11.5
$PaCO_2$ level, kPa	5.70 ± 0.45	5.63 ± 0.43	5.55 ± 0.50	5.57 ± 0.43
PaO_2 level, kPa	13.56 ± 1.26	13.17 ± 1.13	13.22 ± 0.98	13.56 ± 0.83
Eye movement, Hz	1.19 ± 0.10	1.22 ± 0.10	1.00 ± 0.11	1.25 ± 0.10
α-Blockade in the EEG, %	92.20 ± 3.07	89.45 ± 5.03	89.02 ± 4.97	91.08 ± 3.16
% of correct responses	96.90 ± 3.76	75.10 ± 6.57	85.40 ± 11.05	73.80 ± 7.28

Data are the mean ± SD.

Table 2. Significantly activated fields in the motion-form and color-form conditions

Region	Talairach coordinates, mm			Estimated volume, mm³	ΔrCBF$_{ave}$, ml per 100 g per min	ΔrCBF$_{ave}$, % change
	x	*y*	*z*			
Fields activated in the motion-form condition						
Cerebellum L	20	−64	−16	352	14.46 ± 3.50	23.58
Inferior occipital gyrus L	52	−51	−20	396	14.47 ± 3.96	27.52
Inferior occipital gyrus R	−47	−53	−16	396	12.54 ± 3.20	30.65
Lateral occipital gyrus R	−29	−71	−8	440	12.25 ± 2.94	23.44
Lateral occipital gyrus L	50	−53	1	484	11.84 ± 4.13	22.99
Lateral occipital gyrus R	−33	−56	17	352	8.96 ± 2.51	21.44
Fusiform gyrus L	34	−42	−7	528	10.15 ± 3.33	21.00
Lingual gyrus R	−8	−49	4	352	13.09 ± 3.69	27.45
Lingual gyrus/parieto-occipital sulcus, inferior part L	21	−47	4	484	14.08 ± 3.01	35.90
Inferior temporal gyrus R	−46	−45	−8	528	12.49 ± 4.44	29.43
Middle frontal gyrus R	−35	61	−6	440	12.84 ± 3.91	24.87
Middle frontal gyrus L	44	61	6	616	12.47 ± 5.52	21.63
Middle frontal gyrus R	−23	38	20	440	9.12 ± 4.03	35.62
Middle frontal gyrus L	33	40	7	440	7.95 ± 3.74	24.05
Cingulate gyrus, anterior part R	−2	41	20	572	8.39 ± 3.18	25.23
Cingulate gyrus, anterior part L	4	46	21	440	16.12 ± 4.93	22.50
Fields activated in the color-form condition						
Fusiform gyrus R	−27	−33	−23	352	14.37 ± 4.20	27.81
Fusiform gyrus L	42	−11	−22	352	9.44 ± 2.92	18.26
Lateral occipital gyri R	−32	−83	7	572	9.92 ± 3.19	20.34
Lateral occipital gyri R	−23	−72	15	440	9.02 ± 3.46	19.70
Lateral occipital gyri L	18	−82	15	440	11.41 ± 3.93	22.95
Inferior temporal gyrus L	51	−43	6	484	9.60 ± 4.25	23.34
Precuneus L	4	−31	42	352	10.45 ± 3.44	14.62
Intraparietal sulcus L	30	−58	42	528	11.87 ± 2.61	16.99
Precentral gyrus R	−26	−2	51	440	11.46 ± 3.55	19.07
Inferior frontal gyrus R	−23	46	13	484	12.91 ± 2.68	24.33
Superior frontal gyrus L	9	73	−7	352	13.39 ± 3.74	23.63
Cingulate gyrus, mid part R	1	−24	36	352	12.37 ± 6.46	15.15

L, left; R, right.

though to a lesser extent are also present in the temporal and parietal gyri (left inferior temporal gyrus, left precuneus, and left intraparietal sulcus), as well as in the frontal lobe (right inferior and left superior frontal gyri and right precentral gyrus) and the cingulate cortex, indicating that the concerted action of distributed fields accompanies the discrimination of visual forms.

There was an even larger number of distributed fields involved in the discrimination of visual forms based upon motion cues. Most were located in the occipital lobe (fusiform and lingual gyri and inferior and lateral occipital gyri), but there were also fields in the temporal lobe (right inferior temporal gyrus), the prefrontal cortex (both medial frontal gyri), the cingulate cortex, and the cerebellum. In contrast to the other condition, there was no activation in the parietal lobe. Comparing the location of the activated fields in this condition with those present in the perception of visual motion (40), there was no spatial congruence of the fields. This indicates that indeed the motion component *per se* was eliminated by the subtraction of images.

In an earlier experiment, Gulyás and Roland (24) examined those cortical areas involved in the discrimination of visual forms produced by visual textures of different spatial frequencies. Comparing the localization of the fields activated in that experiment with those activated in the present study, we found no overlaps. This observation reinforces the principal

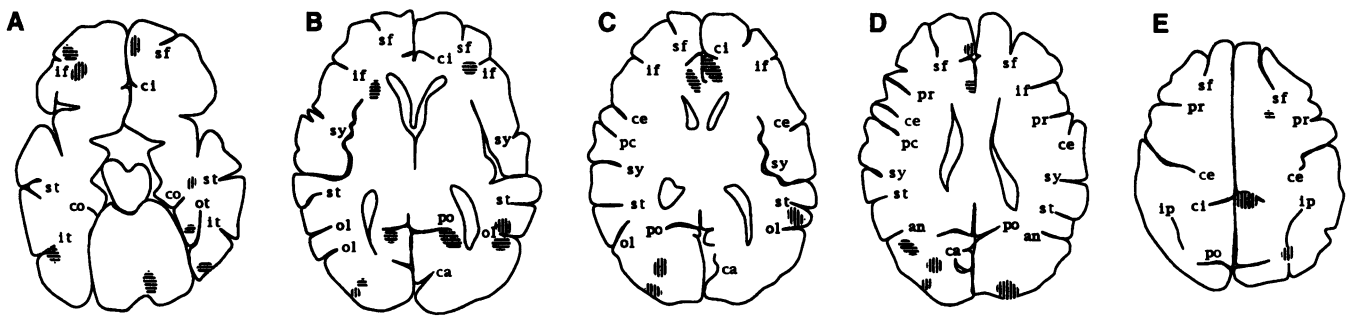

FIG. 3. Cluster images of cortical fields showing significant activation in the color-form (vertical hatching) and motion-form (horizontal hatching) conditions. The images represent horizontal slices, corresponding to the solid oblique lines in Fig. 2. (*A*) Slice 4. (*B*) Slice 7. (*C*) Slice 8. (*D*) Slice 9. (*E*) Slice 11. Left in the images corresponds to the right hemisphere. The contours of the brain, the ventricular system, and major sulci (sf, superior frontal; if, inferior frontal; ci, cingulate; st, superior temporal; it, inferior temporal; co, collateral; ot, occipitotemporal; pr, precentral; ce, central; po, postcentral; po, parietooccipital; ca, calcarine; ol, occipitolateral; sy, Sylvian; an, angular; ip, intraparietal) are taken from the CBA (36, 37, 39).

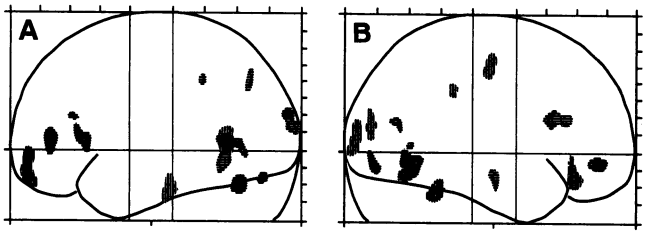

FIG. 4. Activated regions present in the color-form (vertical hatching) and motion-form (horizontal hatching) conditions, expressed in the standard Talairach stereotactic coordinate system (ref. 38; for details, see Fig. 2). Collapsed parasagittal projection. Apparent overlaps in the figure are in fact superpositions that do not overlap in the brain. (*A*) Left hemisphere. (*B*) Right hemisphere.

conclusion of the present study, namely, that the discrimination of visual form can be produced by different cortical networks, depending on the underlying visual submodalities.

Although it remains difficult to relate any of the areas revealed here to any of the many cortical visual areas demonstrated by different methods in monkeys (41), it is interesting to note that inferotemporal lesions in monkeys severely disrupt the learning of a form-from-luminance discrimination without impairing the learning of form from motion (42). A similar dissociation has been reported in brain-damaged human subjects for discriminating forms derived from luminance contrast or from movement (43). These observations and our present findings indicate that different cortical fields participate in the formation and discrimination of form when different visual cues are used to generate this cortical representation. Furthermore, the present findings reinforce the conclusions of recent studies in human subjects on the discrimination of form from motion cues, which engages both occipitotemporal and occipitoparietal regions (44, 45). Our results clearly show coactivation of occipitotemporal and occipitoparietal visual areas during the discrimination of visual form defined by motion or color cues and indicate the functional importance of the anatomical connections between the two visual subsystems (46–48).

We express our gratitude to Mr. W. Pulka and Mr. John Pedersen for their contribution to the experiments. This study was supported by grants from the Wenner-Gren Foundation, the Wenner-Gren Samfundet, the Karolinska Institute, the Human Frontier Science Program Organization, the European Science Foundation, and the United Kingdom Medical Research Council.

1. Ramachandran, V. S. & Gregory, R. L. (1975) *Nature (London)* **275**, 55–56.
2. Zeki, S. (1974) *J. Physiol. (London)* **236**, 549–573.
3. Zeki, S. (1980) *Nature (London)* **284**, 412–418.
4. Livingstone, M. S. & Hubel, D. M. (1987) *J. Neurosci.* **3**, 3416–3468.
5. Livingstone, M. S. & Hubel, D. H. (1988) *Science* **240**, 740–749.
6. Schiller, P. H., Logothetis, N. K. & Charles, E. R. (1990) *Nature (London)* **343**, 68–70.
7. Schiller, P. H. (1993) in *Functional Organisation of the Human Visual System*, eds. Gulyás, B., Ottoson, D. & Roland, P. E. (Pergamon, Oxford), pp. 43–58.
8. Ramachandran, V. S. (1987) *Nature (London)* **328**, 645–647.
9. Cavanagh, P. & Anstis, S. (1991) *Vision Res.* **31**, 2109–2148.
10. Papathomas, T. V., Gorea, A. & Julesz, B. (1991) *Vision Res.* **31**, 1883–1891.
11. Carney, T., Shadlen, M. & Switkes, E. (1987) *Nature (London)* **328**, 647–649.
12. DeYoe, E. A. & Van Essen, D. C. (1988) *Trends Neurosci.* **11**, 219–226.
13. Gross, C. G., Rocha-Miranda, C. E. & Bender, D. B. (1972) *J. Neurophysiol.* **35**, 96–111.
14. Perrett, D. I., Rolls, E. T. & Caan, W. (1982) *Exp. Brain Res.* **47**, 329–343.
15. Schwartz, E. L., Desimone, R., Albright, T. D. & Gross, C. G. (1983) *Proc. Natl. Acad. Sci. USA* **80**, 5776–5778.
16. Gross, C. G., Desimone, R., Albright, T. D. & Schwartz, E. L. (1985) *Pontif. Acad. Sci. Scr. Varia* **54**, 179–201.
17. Desimone, R. (1991) *J. Cognit. Neurosci.* **3**, 1–8.
18. Sáry, Gy., Vogels, R. & Orban, G. A. (1993) *Science* **260**, 995–997.
19. Heywood, C. A. & Cowey, A. (1992) *Philos. Trans. R. Soc. London B* **335**, 31–38.
20. Roland, P. E., Gulyás, B., Seitz, R. J., Bohm, C. & Stone-Elander, S. (1990) *NeuroReport* **1**, 53–56.
21. Gulyás, B. & Roland, P. E. (1991) *NeuroReport* **2**, 585–588.
22. Corbetta, M., Miezin, F. M., Dobmeyer, S., Shulman, G. L. & Petersen, S. E. (1991) *J. Neurosci.* **11**, 2383–2402.
23. Sergent, J., Ohta, S. & MacDonald, B. (1992) *Brain* **115**, 15–36.
24. Gulyás, B. & Roland, P. E. (1994) *Eur. J. Neurosci.*, in press.
25. World Medical Association (1964) *Declaration of Helsinki, Code of Ethics*, 12 July 1964, *Br. Med. J.*
26. Code of Federal Regulations (1989) *Protection of Human Subjects*, Title 45, Part 46.
27. Oldfield, R. C. (1971) *Neuropsychologia* **9**, 97–113.
28. Velhagen, K. (1964) *Tafeln zur Prüfung des Farbensinnes* (Thieme, Stuttgart, F.R.G.).
29. Greitz, T., Bergström, M., Boëthius, J., Kingsley, D. & Ribbe, T. (1980) *Neuroradiology* **19**, 1–6.
30. Bergström, M., Boëthius, J., Eriksson, L., Greitz, T., Ribbe, T. & Widén, L. (1981) *J. Comput. Assist. Tomogr.* **5**, 136–141.
31. Litton, J. E., Holte, S. & Eriksson, L. (1990) *IEEE Trans. Nucl. Sci.* **37**, 743–748.
32. Evans, A. C., Thompson, C. J., Marrett, S., Meyer, E. & Mazza, M. (1991) *IEEE Trans. Med. Imaging* **10**, 90–98.
33. Berridge, M. S., Adler, L. P., Nelson, A. D., Cassidy, E. H., Muzic, R. F., Bednarczyk, E. M. & Miraldi, F. (1991) *J. Cereb. Blood Flow Metab.* **11**, 707–715.
34. Olesen, J., Paulson, O. & Lassen, N. A. (1971) *Stroke* **2**, 519–540.
35. Roland, P. E., Levin, B., Kawashima, R. & Åkerman, S. (1993) *Hum. Brain Mapping* **1**, 3–19.
36. Greitz, T., Bohm, C., Holte, S. & Eriksson, L. (1991) *J. Comput. Assist. Tomogr.* **15**, 26–38.
37. Seitz, R. J., Bohm, C., Greitz, T., Roland, P. E., Eriksson, L., Blomqvist, G., Rosenqvist, G. & Nordell, B. (1990) *J. Cereb. Blood Flow Metab.* **10**, 443–457.
38. Talairach, J., Szikla, G., Tournoux, P., Prossalentis, A., Bordas-Ferrer, M., Covello, L., Iacob, M. & Mempel, E. (1967) *Atlas d'Anatomie Stéréotaxique du Télencéphale* (Masson, Paris).
39. Greitz, T., Bohm, C., Holte, S. & Eriksson, L. (1991) *J. Comput. Assist. Tomogr.* **15**, 26–38.
40. Zeki, S., Watson, J. D. G., Lueck, C. J., Friston, K. J., Kennard, C. & Frackowiak, R. S. J. (1991) *J. Neurosci.* **11**, 641–649.
41. Van Essen, D. C. (1985) in *Cerebral Cortex: Visual Cortex*, eds. Peters, A. & Jones, E. G. (Plenum, New York), Vol. 3, pp. 259–329.
42. Britten, K. H., Newsome, W. T. & Saunders, R. C. (1992) *Exp. Brain Res.* **88**, 292–302.
43. Vaina, L. M., Lemay, M., Bienfang, D. C., Choi, A. Y. & Nakayama, K. (1990) *Vis. Neurosci.* **5**, 353–369.
44. Regan, D., Giaschi, D., Sharpe, J. A. & Hong, X. H. (1992) *J. Neurosci.* **12**, 2198–2210.
45. Lassonde, M., Faubert, J., Schiavetto, A. & Bilodeau, L. (1993) *Invest. Ophthalmol. Visual Sci.* **34**, 795 (abstr.).
46. Boussaoud, D., Ungerleider, L. G. & Desimone, R. (1990) *J. Comp. Neurol.* **296**, 462–495.
47. Morel, A. & Bullier, J. (1991) *Vis. Neurosci.* **4**, 555–578.
48. Van Essen, D. C., Anderson, C. H. & Felleman, D. J. (1992) *Science* **255**, 419–423.